JOC The Journal of Organic Chemistry

Article

pubs.acs.org/joc

Fluorescence-Enhanced Chemosensor for Metal Cation Detection Based on Pyridine and Carbazole

Xin Jiang Feng,*[,†] Pin Zhan Tian,[†] Zheng Xu,*[,†] Shao Fu Chen,[†] and Man Shing Wong*[,‡]

[†]Key Laboratory of Organosilicon Chemistry and Material Technology of the Ministry of Education, Hangzhou Normal University, Hangzhou 310012, P. R. China

[‡]Department of Chemistry and Institute of Advanced Materials, Hong Kong Baptist University, Kowloon Tong, Hong Kong SAR, China

Supporting Information

ABSTRACT: A series of donor−acceptor systems incorporating a carbazole moiety as the donating unit and pyridine moiety as the accepting unit have been designed and synthesized. The spectroscopic and electrochemical behaviors of the carbazole derivatives demonstrate that the carbazole unit interacts with the electron-accepting group through the π-conjugated spacer, thus leading to the intramolecular charge transfer (ICT). The pyridine-substituted carbazole derivatives show significant sensing and coordinating properties toward a wide range of metal cations. Compound **S2** exhibits fluorescence enhancement upon association with transition metal cations, and compound **V3** shows high selectivity for Cu^{2+} among this series of materials. DFT calculations indicate the different association abilities of the dyes and the enhancement of ICT upon addition of the metal cations.

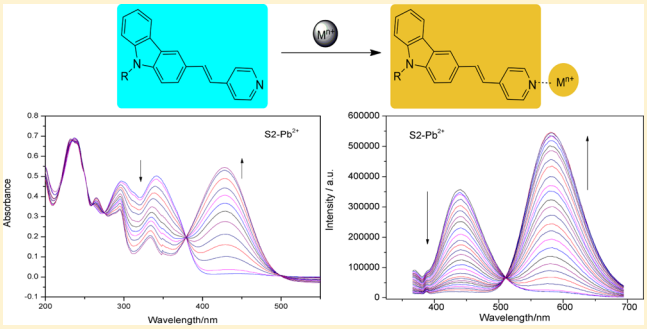

INTRODUCTION

Heavy metal ion contamination poses significant risks to environmental systems. As a result, the design and synthesis of chemosensors with high selectivity and sensitivity for heavy metal ions is a domain of wide interest.[1−9] Among the detection approaches, fluorescence spectroscopy is widely used because of its high sensitivity, simple application, and low-cost instrumentation. However, fluorescent sensors for heavy metal ions have remained rare to date[10−13] because heavy metal ions are known to quench fluorescence emission via enhanced spin−orbit coupling[14] or energy or electron transfer.[15] On the other hand, communication between the donor (D) and acceptor (A) in donor−acceptor (D−A) molecules has been studied widely,[1,4,16−19] and detection of heavy metal cations by spectroscopic and electrochemical methods in such studies has been reported.

Recently, carbazole derivatives have been shown to be promising materials for two-photon applications[20−22] and molecular assembly.[23] The carbazole moiety plays the role of the donor in various D−A systems and can be easily functionalized by classical reactions including Heck cross-coupling, Sonogashira cross-coupling, and Wittig−Horner reactions.[24−27] Also, pyridine-related π-conjugated derivatives with donor−acceptor properties involving the lone-pair electrons on the pyridine nitrogen have been used as heavy metal sensors.[2] Pyridine can constitute π-conjugated donor−acceptor molecules when coupled with carbazole by different π-conjugated linkers. Methylated salts of carbazole and pyridine derivatives exhibited multiphoton absorption properties and interaction with biological systems in our previous research.[28] We think that the intramolecular charge transfer (ICT) in neutral compounds of this kind could be tuned by the modification of the conjugated cores and the molecule dimensions. Furthermore, changes in ICT induced by metal cation binding could exhibit spectroscopic responses, which could enable the use of these dyes as chemosensors.

In this work, the synthesis of carbazole−pyridine derivatives by Heck coupling and the Wadsworth−Emmons reaction is described. Elongating the bridging unit by inserting an aryl ring or changing the molecule dimensions gives rise to a change in ICT. The interaction of carbazole−pyridine derivatives with an external stimulus of metal cations can tune the ICT, resulting in remarkable changes in absorption spectra, fluorescence spectra, ^{1}H NMR spectra, and electrochemical properties. Geometry optimizations and orbital energies of the dyes and two metal-associated species were calculated by density functional theory (DFT).

RESULTS AND DISCUSSION

Synthesis. Heck coupling and the Wadsworth−Emmons reaction were used to synthesize the carbazole−pyridine derivatives. Their syntheses are outlined in Scheme 1. Palladium-catalyzed Heck coupling of **1a** and **1b** with 4-

Received: August 24, 2013
Published: October 30, 2013

Scheme 1. Syntheses of S2, V2, S3, and V3

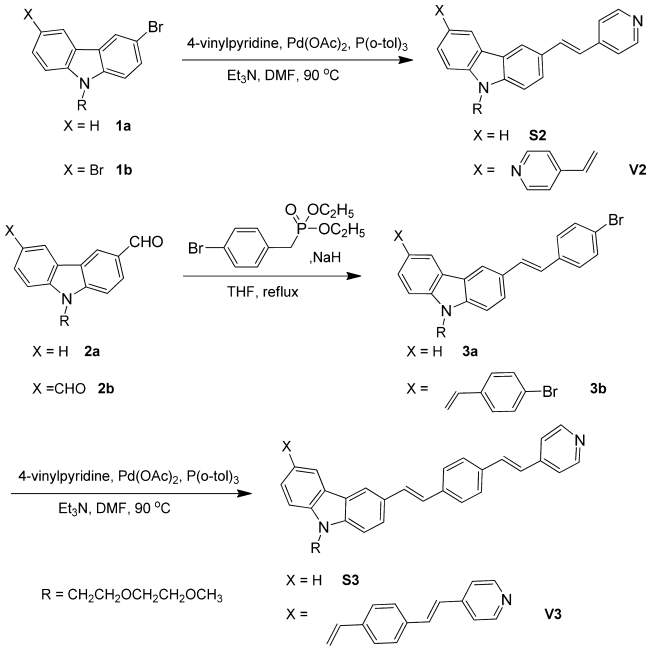

vinylpyridine using $Pd(OAc)_2/2P(o\text{-tolyl})_3$ as a catalyst afforded **S2** and **V2** in yields of 67% and 78%, respectively. Wadsworth–Emmons reaction of **2a** and **2b** with diethyl 4-bromobenzylphosphonate gave **3a** and **3b** in moderate to good yields of 61% and 83%, respectively. **S3** and **V3** were prepared via Heck coupling of **3a** and **3b** with 4-vinylpyridine in good yields of 84% and 74%, respectively.

Photophysical Properties. The photophysical characteristics of the new oligomers **S2**, **V2**, **S3**, and **V3** were examined by UV–vis and fluorescence spectroscopy. The absorption and fluorescence spectra of these oligomers are depicted in Figure 1 and Figures 1S and 2S in the Supporting Information, and the spectral data are summarized in Table 1. In view of the absorption spectra obtained in toluene, chloroform, and acetonitrile, all of the oligomers have similar absorption spectral features, which are basically composed of two major absorption bands. The shorter-wavelength absorption peak appears around 300 nm and is assigned to the n → π^* transition of the carbazole moiety, while the lower-energy absorption peaked at 338–399 nm arises from the $\pi \rightarrow \pi^*$ transition of the π-conjugated core. In general, the absorption spectra of these oligomers do not exhibit significant solvatochromic effects. On the contrary, the fluorescence spectra are solvent-dependent, exhibiting less or no vibronic structure and large red shifts with increasing solvent polarity. For instance, the emission maxima of **S3** exhibit solvatochromic shifts of 33 and 37 nm when the solvent is changed from toluene to chloroform and from chloroform to acetonitrile, respectively (Figure 2). Furthermore, the solvatochromatic effect is much larger for the chromophores with longer conjugation lengths than for the lower homologues, indicating that the electronic communication between the carbazole moiety and the pyridine moiety can be optimized by varying the conjugation length.

Electrochemical Properties. To probe the redox properties of the carbazole-based π-conjugated chromophores, cyclic voltammetry (CV) was carried out in a three-electrode cell setup with 0.1 M Bu_4NPF_6 as a supporting electrolyte in CH_2Cl_2. The HOMO and LUMO energies of these compounds were calculated from the oxidation and reduction potentials and are listed in Table 1. Comparison of **S2** with **S3** and **V2** with **V3** showed that E_{HOMO} increases and E_{LUMO} decreases with increasing conjugation length, indicating that the energy gap of this series of molecules can be tuned by varying the conjugation length. Such changes in the energy gap could be attributed to the ICT, which in turn could tune the binding affinity of the nitrogen on the pyridine ring to metal cations.

Metal Cation Association Study. ^{1}H NMR, UV–vis, and fluorescence spectroscopic titrations and cyclic voltammetry were used to evaluate the binding properties of the compounds toward various metal ions in acetonitrile.

Binding Properties: ^{1}H NMR Titrations. ^{1}H NMR titrations were performed in 5×10^{-4} M acetonitrile-d_3 with addition of a 5×10^{-2} M solution of $Pb(ClO_4)_2$ in acetonitrile-d_3. The chemical shifts of the resonances associated with the pyridyl protons in the ^{1}H NMR spectrum changed significantly upon complexation with Pb^{2+} ion. The signals of all the protons in the carbazole moiety shifted downfield, but the shifts were small compared with that of the proton at the 3-position of the pyridyl ring (Figure 3 and Figures S3 and S4 in the Supporting Information). The maximum chemical shifts of H-3 on the pyridyl ring were 0.531, 0.557, and 0.437 ppm for **S2**, **S3**, and **V2**, respectively (**V3** dissolved too poorly in acetonitrile for an NMR titration to be performed). These observations confirm that Pb^{2+} interacts with the nitrogen atom on the pyridyl group, thus leading to the ICT in these molecules.

The variation of ^{1}H NMR spectra upon titration with Pb^{2+} and the plots of normalized change of chemical shift versus cation molar fraction (Figure S5 in the Supporting Information) show that **S2** and **S3** exhibited saturation of the

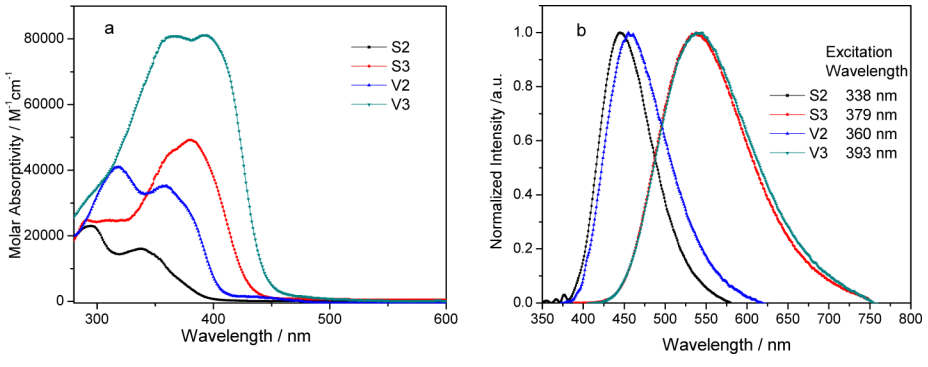

Figure 1. (a) Absorption and (b) fluorescence spectra of chromophores **S2**, **S3**, **V2**, and **V3** in CH_3CN.

dx.doi.org/10.1021/jo401808c | J. Org. Chem. 2013, 78, 11318–11325

Table 1. Summary of Linear Optical Measurements of Neutral Carbazole-Based Chromophores in Various Solvents

	toluene		chloroform		acetonitrile				
	λ_{max}^{abs} (λ_{max}^{em}) (nm)	Φ_{FL} [a]	λ_{max}^{abs} (λ_{max}^{em}) (nm)	Φ_{FL} [a]	λ_{max}^{abs} (λ_{max}^{em}) (nm)	Φ_{FL} [a]	E_{HOMO} (eV) [c]	E_{LUMO} (eV) [c]	T_{dec} (°C) [d]
S2	341 (412)	0.012 [b]	342 (433)	0.012 [b]	338 (445)	0.043 [b]	−5.32	−3.16	–
S3	387 (468)	0.48	387 (501)	0.57	379 (538)	0.48	−5.23	−3.18	439
V2	360 (408)	0.086 [b]	364 (436)	0.055 [b]	360 (455)	0.093 [b]	−5.31	−3.14	436
V3	398 (450)	0.26	399 (499)	0.46	393 (545)	0.20	−5.24	−3.25	436

[a]Using quinine sulfate monohydrate (Φ_{350} = 0.58) as a standard. [b]Averages of two independent measurements. [c]Estimated from CV measurements. [d]Determined using a thermogravimetric analyzer with a heating rate of 20 °C/min under N_2.

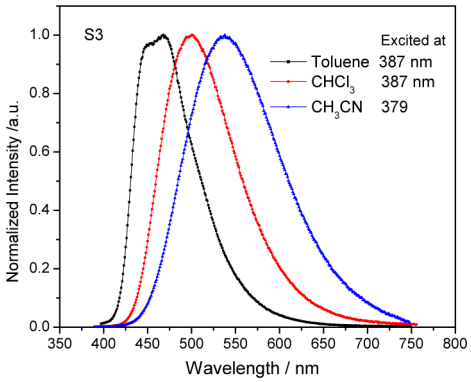

Figure 2. Solvatochromic effect of **S3** in toluene, chloroform, and acetonitrile.

change in chemical shift when 1 equiv of Pb^{2+} ion was added, while **V2** exhibited saturation of the change in chemical shift when 2 equiv of Pb^{2+} ion were added, which implies that every nitrogen on a pyridyl ring in all three compounds associates with one Pb^{2+} ion. Furthermore, Job's plots of the change in proton chemical shift upon molar equivalent addition of $Pb(ClO_4)_2$ also indicated the 1:1 stoichiometries of the complexes between **S2** or **S3** and $Pb^{2+}$and the 1:2 stoichiometry of the complex between **V2** and Pb^{2+} (Figure S6 in the Supporting Information)

The 1:1 stoichiometry for binding of Pb^{2+} ion by **S2** and **S3** was also evidenced by the close agreement of the experimental data with the theoretical fit according to the Hildebrand equation (eq 1):[29]

$$\frac{\delta_0}{\delta_0 - \delta} = \frac{\delta_0}{nC_0} + \frac{\delta_0}{nC_0K_s}\left(\frac{1}{[M]}\right) \quad (1)$$

where δ and δ_0 are the chemical shifts for proton in the presence and absence of metal ion, respectively, n is the ratio of the dye and Pb^{2+} ion, C_0 is the dye concentration, K_s is the binding constant, and [M] is the concentration of the Pb^{2+} ion. The binding constants for **S2** and **S3** are 3.12×10^5 and 1.89×10^5 M^{-1}, respectively. The fact that the binding constant for **S2** is larger than that for **S3** indicates that **S2** exhibits stronger affinity than **S3** when binding to Pb^{2+} ion. The result also shows that ICT in carbazole−pyridine compounds can be tuned by varying the conjugation length, thus leading to different affinities for association with metal cations.

Binding Properties: Cyclic Voltammetry. The progressive addition of $Pb(ClO_4)_2$ to solutions of **S2**, **S3**, and **V2** in CH_3CN in the presence of n-Bu_4NPF_6 caused significant modification of the oxidation potentials in CVs, with substantial positive shifts of the first oxidation potential from 647 to 872 mV, 519 to 620 mV, and 652 to 881 mV for **S2**, **S3**, and **V2**, respectively (Figure 4 and Figure S7 in the Supporting Information). However, data for **V3** could not be obtained because of its poor solubility in acetonitrile. The positive shifts of the first oxidation potentials arise from the reduced electron density located in the carbazole moiety because of increased ICT upon binding of the pyridine nitrogen with Pb^{2+} ion. On the other hand, **S2** and **S3** showed saturation of the positive shift when 1 equiv of Pb^{2+} was added, while **V2** showed saturation of the positive shift when 2 equiv of Pb^{2+} was added. The results also indicate that metal cation is complexed by only the nitrogen atoms on pyridine rings and that one pyridyl nitrogen associates with one metal cation in solution. The more

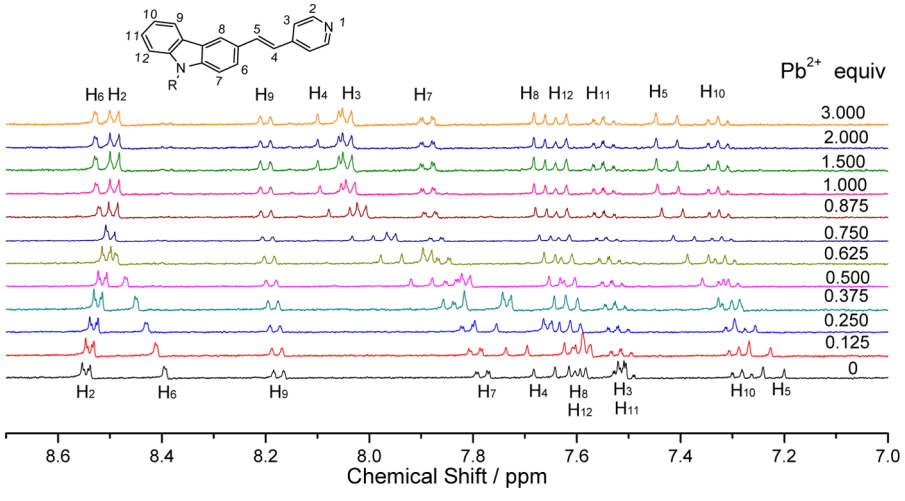

Figure 3. NMR titration of **S2** with $Pb(ClO_4)_2$ in 0.5 mM acetonitrile-d_3 solution.

dx.doi.org/10.1021/jo401808c | J. Org. Chem. 2013, 78, 11318−11325

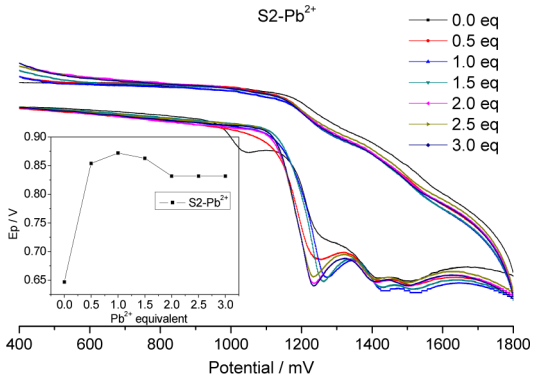

Figure 4. CV titration of **S2** in acetonitrile and (inset) plot of E_p vs equivalents of metal.

highly conjugated compound (**S3**) shows less change in the first oxidation potential (ΔE^1_{ox}) than do the less conjugated compounds **S2** and **V2**, indicating that the ICT in the dye induced upon the stimulus of Pb^{2+} decreases with elongation of the conjugated core. Also, **V2** shows a ΔE^1_{ox} value slightly larger than that for **S2**, which indicates that the binding of the second Pb^{2+} results in further ICT in **V2**. However, the influence on the first oxidation by the second binding of Pb^{2+} is much smaller than that induced by the first binding of Pb^{2+}. These results also indicate that upon binding to Pb^{2+}, the ICT in these carbazole pyridine derivatives can be modified by varying the conjugated core length or molecular dimensions.

Binding Properties: UV–Vis Titrations. To scan the metal cation binding properties of these materials, UV–vis titrations of carbazole derivative **S2** with a wide range of cationic solutions (Na^+, Mg^{2+}, Ca^{2+}, Zn^{2+}, Ag^+, Cd^{2+}, Hg^{2+}, and Pb^{2+}) were performed by the progressive introduction of the corresponding metal perchlorate solution into a 5 μm solution of the 4-pyridyl derivative **S2** in CH_3CN (Figure 5 and Figure S8 in the Supporting Information). As can be seen, among the metal ions tested, no significant spectral changes were observed for Na^+, Mg^{2+}, Ca^{2+}, Ag^+, and Cd^{2+}, while moderate to significant spectral changes were observed for Zn^{2+}, Hg^{2+}, and Pb^{2+}. Taking Pb^{2+} for an example, the resulting electronic spectra clearly show the appearance of a new low-energy band centered around 435 nm that increases with the progressive addition of lead perchlorate at the expense of the initial ICT band at 338 nm. This progressive change in the spectrum revealed isosbestic points at 257, 278, and 379 nm, correlated to the presence of only two species in equilibrium in solution, namely, the free ligand **S2** and the **S2**·Pb^{2+} complex. Binding of the Pb^{2+} cation by the pyridyl unit is therefore accompanied by a spectacular red shift of the ICT band of 97 nm, illustrating that the electron-accepting ability of the pyridyl moiety is increased once it is coordinated to a cation, leading to a lowering of the energy of the ICT band.

Binding Properties: Fluorescence Titrations. Since fluorescence response is usually more sensitive than UV–vis absorption, the binding and sensing properties of these dyes were also investigated by fluorescence titrations of 1 μm solutions in acetonitrile with various metal cations, including Na^+, Ag^+, Ca^{2+}, Mg^{2+}, Zn^{2+}, Cd^{2+}, Cu^{2+}, Hg^{2+}, and Pb^{2+} (Figure 6 and Figures S9 and S10 in the Supporting Information). Upon titration of **S2** in acetonitrile with various cations, very small or no significant spectral changes were observed for Na^+, Mg^{2+}, Ca^{2+}, Cd^{2+}, and Ag^+, while the fluorescence spectra changed significantly for Zn^{2+}, Cu^{2+}, Hg^{2+}, and Pb^{2+}. Taking Pb^{2+} for an example, the peak centered at 445 nm decreased progressively and an obvious emission band slowly emerged at around 575 nm. The peak around 445 nm arises from the ICT of the neutral species. Upon the addition of metal ions, the concentration of this species decreased, giving rise to the decrease in fluorescence intensity around 445 nm. The emission at 575 nm can be assigned to the emission of the new species generated by the binding of **S2** and Pb^{2+}. Moreover, the fluorescence intensity at 575 nm was stronger than the original emission of the neutral species **S2**, which implies that the new species is a stronger fluorescent chromophore than the neutral one. As a result, **S2** can be a fluorescence-enhanced detector for heavy metal cations. However, the dyes **V2**, **S3**, and **V3** exhibited only fluorescence quenching upon addition of metal ions. This could be attributed to the fact that the new complex species of **V2**, **S3**, and **V3** upon association with metal cations exhibit no fluorescence or very weak fluorescence. Both **V2** and **S3** show selectivity for Cu^{2+} and Hg^{2+} cations, while **V3** exhibits high selectivity for Cu^{2+} among the tested ions (Figure 7). The four dyes show different affinities and selectivities for metal cations, with **S2** exhibiting the largest affinities for metal cations and **V3** showing the smallest affinities. The results indicate that increasing the conjugation length and the dimensions of the dyes decreases the binding affinity of the pyridine nitrogen to metal cation. All of these facts suggest that these dyes can be candidates for cation sensors for transition metals and that the affinity can be tuned by varying the conjugation length and dimension of the molecules.

Theoretical Calculations. In order to investigate the relationship between the compounds' optical and charge-

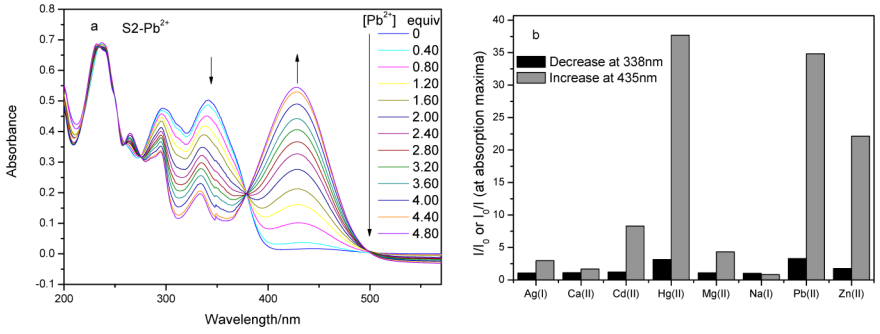

Figure 5. (a) Absorption spectra of **S2** upon progressive addition of Pb^{2+} and (b) **S2** absorbance intensity changes upon addition of 3 equiv of metal ions in acetonitrile.

dx.doi.org/10.1021/jo401808c | J. Org. Chem. 2013, 78, 11318–11325

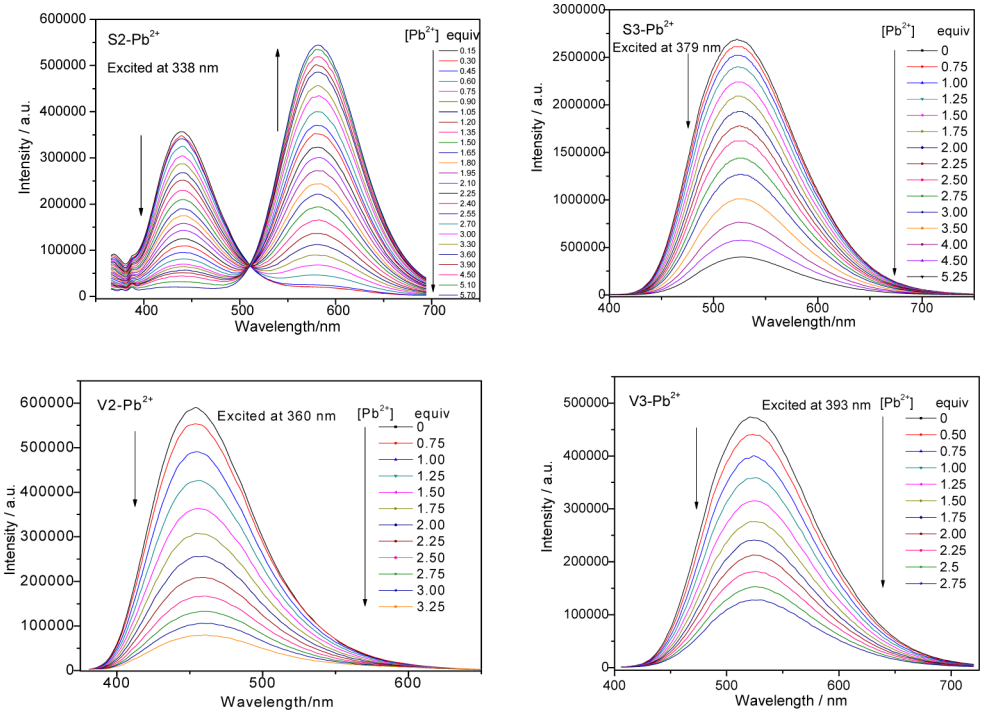

Figure 6. Fluorescence spectra of **S2**, **S3**, **V2**, and **V3** upon progressive addition of Pb^{2+} in acetonitrile.

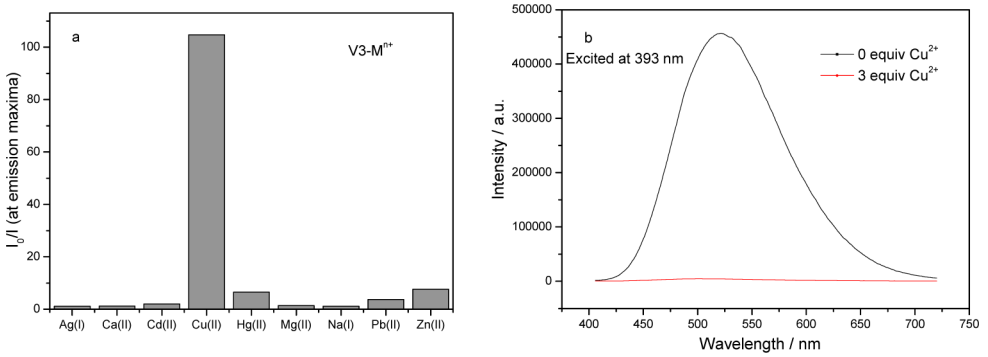

Figure 7. (a) Fluorescence intensity changes of **V3** upon addition of 3 equiv of metal ions in acetonitrile. (b) Fluorescence spectra of **V3** before and after addition of 3 equiv of Cu^{2+} in acetonitrile.

transfer properties and the molecular structure and complexation state with metal cations, DFT and TD-DFT calculations were carried out on the four dyes (**S2**, **V2**, **S3**, and **V3**) and two metal complexes (**S2**·Cu^{2+} and **V3**·Cu^{2+}) using the Gaussian 09 program.[30] The B3LYP functional in combination with the 6-31G(d,p) basis set for C, N, and H and the LANL2DZ basis set for Cu was used for all of the calculations. It should be noted that the alkyl chain on the carbazole nitrogen was simplified as ethyl in all of the calculations.

The frontier molecular orbitals (HOMO and LUMO) for all of the studied compounds, including the two metal complexes, are shown in Figure 8. First, it can be seen that the HOMO of **S2** is delocalized throughout the backbone, including the electron-withdrawing pyridine ring. When the molecular structure is shifted from **S2** to **V2**, **S3**, and **V3**, the contribution from the pyridine ring gradually decreases in the series, and no apparent contribution from the pyridine moiety is observed for **V3**. This decreasing contribution of the pyridine ring to the HOMO is supposed to be related to a decrease of the affinity of the pyridine N lone pair to the metal cation, which accords well with our experimental findings that the association ability of the dyes decreases with increasing conjugation length and molecular dimensions. Second, a brief comparison of the HOMO and LUMO shapes of corresponding compounds shows that the main ICT mode for the four dyes can be considered to go from the carbazole moiety to the pyridine moiety, and the complexation of the Cu^{2+} cation causes a modification of the ICT mode: the Cu^{2+} plus pyridine moiety becomes the accepting part for **S2**·Cu^{2+}, while Cu^{2+} is the only accepting part for **V3**·Cu^{2+}. This may be why **S2** exhibits fluorescence enhancement and **V3** shows fluorescence quenching toward metal cations.

In addition, TD-DFT calculations based on the optimized structures of **S2**, **V2**, **S3**, **V3** were carried out to obtain the wavelengths of the transitions for HOMO to LUMO excitations together with the oscillator strengths (*f*, listed in Figure 8). A gradual increase in the wavelength of the transition for the HOMO to LUMO excitation was observed for the series **S2**, **V2**, **S3**, and **V3** with wavelengths of 390.8, 444.0, 470.1, and 510.4 nm, respectively, which is consistent with the

dx.doi.org/10.1021/jo401808c | J. Org. Chem. 2013, 78, 11318−11325

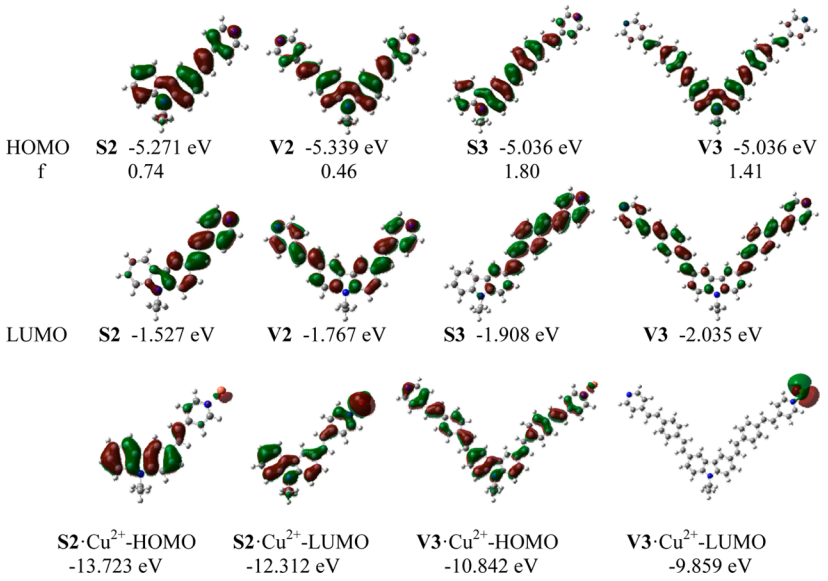

Figure 8. Frontier molecular orbitals of **S2**, **V2**, **S3**, **V3**, **S2**·Cu^{2+}, and **V3**·Cu^{2+}.

trend of the absorption maxima measured in UV−vis measurements in solution.

CONCLUSION

A series of carbazole derivatives conjugated with pyridine by a π-conjugated core was synthesized via Heck coupling and the Wadsworth−Emmons reaction. Spectroscopic, electrochemical, and metal-cation-binding studies demonstrate that this series of chromophores can communicate electrons between carbazole and pyridine moieties through the π-conjugated cores, thus leading to intramolecular charge transfer. The interaction of carbazole derivatives with metal ions can significantly modulate the ICT state, resulting in remarkable changes in UV−vis and fluorescence spectra, proton chemical shifts, and cyclic voltammograms. Among this series of materials, **S2** exhibits fluorescence enhancement upon association with the heavy metal cations and **V3** shows high selectivity for Cu^{2+}. The affinity of the pyridine N lone pair decreases with increasing conjugation length and molecular dimensions. DFT calculations on **S2**, **V2**, **S3**, **V3**, **S2**·Cu^{2+}, and **V3**·Cu^{2+} also indicate the different association abilities of the dyes and the enhancement of ICT upon addition of the metal cations. Fluorescence enhancement of **S2** and quenching of **V3** are also revealed by electronic structures of their metal complexes. Our findings indicate that these materials can be candidates for heavy metal ion detectors and that the affinity of these materials upon association with metal cations can be tuned by varying the conjugation length and molecular dimensions.

EXPERIMENTAL SECTION

Materials and Reagents. Compounds **1a**, **1b**, **2a**, and **2b** were prepared according to the procedures in our previous research.[28] Tetrahydrofuran was used after refluxing for 2−3 h in the presence of sodium. Other reagents were of chemical or analytical grade and were used as received.

*Compound **S2**.* To a solution of compound **1a** (0.50 g, 1.44 mmol), palladium acetate (17 mg, 0.07 mmol) and tri-*o*-tolylphosphine (43 mg, 0.14 mmol) in triethylamine (2 mL) and DMF (6 mL) was added 4-vinylpyridine (0.31 mL, 2.87 mmol) under N_2. The reaction mixture was stirred at 120 °C overnight. Water was added, and then the reaction mixture was extracted with DCM. The combined organic layers were washed with brine, dried over sodium sulfate, and evaporated in vacuum to afford a brown oil that was purified via silica gel column chromatography using methanol/dichloromethane (0−3%) as an eluent, affording 358 mg (67% yield) of **S2** as a light-yellow viscous liquid. ^{1}H NMR (400 MHz, $CDCl_3$, δ): 8.53 (d, J = 5.6 Hz, 2H), 8.18 (d, J = 1.6 Hz, 1H), 8.08 (d, J = 7.6 Hz, 1H), 7.62 (dd, J = 8.4 Hz, 1.60 Hz, 1H), 7.47 (m, 4H), 7.33 (d, J = 6.0 Hz, 2H), 7.25 (m, 1H), 7.00 (d, J = 16.4 Hz, 1H), 4.45 (t, J = 6.0 Hz, 2H), 3.83 (t, J = 6.0 Hz, 2H), 3.48 (m, 2H), 3.39 (m, 2H), 3.29 (s, 3H). ^{13}C NMR (100 MHz, $CDCl_3$, δ): 149.9, 145.1, 140.8, 134.0, 127.3, 126.0, 124.6, 123.1, 122.9, 122.7, 120.4, 120.2, 119.4, 119.2, 109.2, 109.0, 71.8, 70.7, 69.1, 58.9, 43.1. HRMS (MALDI-TOF) m/z: $[M]^+$ calcd for $C_{24}H_{24}N_2O_2$ 372.1832, found 372.1835.

*Compound **V2**.* To a solution of compound **1b** (500 mg, 1.17 mmol), palladium acetate (25 mg, 0.11 mmol), and tri-*o*-tolylphosphine (67 mg, 0.22 mmol) in triethylamine (3 mL) and DMF (9 mL) was added 4-vinylpyridine (0.5 mL, 6.68 mmol) under N_2. The mixture was stirred at 110 °C overnight. Water was added, and then the reaction mixture was extracted with DCM. The combined organic layers were washed with brine, dried over anhydrous sodium sulfate, and evaporated to dryness. The residue was turned into a brown solid under vacuum, which was further precipitated by DCM and petroleum ether. The product was then purified by silica gel column chromatography using methanol/dichloromethane (0−3%) as an eluent, affording 434 mg (78% yield) of **V2** as a yellow solid. ^{1}H NMR (400 MHz, $CDCl_3$, δ): 8.56 (d, J = 6.4 Hz, 4H), 8.26 (d, J = 1.6 Hz, 2H), 7.68 (dd, J = 8.4 Hz, 1.6 Hz, 2H), 7.48 (m, 4H), 7.40 (dd, J = 4.8 Hz, 1.6 Hz, 4H), 7.06 (d, J = 16.0 Hz, 2H), 4.51 (t, J = 6.4 Hz, 2H), 3.88 (t, J = 6.0 Hz, 2H), 3.51 (m, 2H), 3.41 (m, 2H), 3.29 (s, 3H). ^{13}C NMR (100 MHz, $CDCl_3$, δ): 150.0, 145.1, 141.3, 133.8, 127.9, 125.2, 123.4, 123.2, 120.5, 119.3, 109.6, 71.9, 70.8, 69.2, 43.4. HRMS (MALDI-TOF) m/z: $[M]^+$ calcd for $C_{31}H_{29}N_3O_2$ 474.2302, found 474.2305. Anal. Calcd for $C_{31}H_{29}N_3O_2$: C, 78.29; H, 6.15; N, 8.84. Found: C, 78.49; H, 6.14; N, 8.71.

*Compound **3a**.* To a solution of compound **2a** (1.30 g, 4.2 mmol) in dry THF was added sodium hydride (200 mg, 60% in mineral oil, 5.0 mmol). The resulting mixture was stirred for 40 min at 45 °C, and diethyl 4-benzylphosphonate (0.84 g, 2.8 mmol) in THF was added via syringe. The solution was then heated to reflux and stirred overnight. The reaction mixture was cooled to room temperature and quenched with aqueous ammonium chloride. The organic layer was separated and dried over anhydrous sodium sulfate. The solvent was removed in vacuo, and the residue was recrystallized from dichloromethane and hexane to give 600 mg (61% yield) of compound **3a** as a brown solid. ^{1}H NMR (400 MHz, $CDCl_3$, δ): 8.18 (d, J = 1.6 Hz, 1H), 8.09 (d, J = 7.6 Hz, 1H), 7.63 (dd, J = 8.4 Hz, 2.0 Hz, 1H), 7.38−7.47

dx.doi.org/10.1021/jo401808c | J. Org. Chem. 2013, 78, 11318−11325

(m, 7H), 7.35 (d, J = 16.4 Hz, 1H), 7.22 (m, 1H), 7.05 (d, J = 16.4 Hz, 1H), 4.50 (t, J = 6.4 Hz, 2H), 3.85 (t, J = 6.4 Hz, 2H), 3.50 (m, 2H), 3.41 (m, 2H), 3.29 (s, 3H). ^{13}C NMR (100 MHz, $CDCl_3$, δ): 140.9, 140.5, 136.8, 131.6, 130.3, 128.3, 127.6, 125.9, 124.7, 124.4, 123.2, 122.8, 120.5, 120.3, 119.3, 118.6, 109.1, 109.0, 71.9, 70.8, 69.2, 59.0, 43.2. HRMS (MALDI-TOF) m/z: $[M]^+$ calcd for $C_{25}H_{24}BrNO_2$ 449.0985, found 449.0978.

Compound ***S3***. A mixture of compound **3a** (0.57 g, 1.27 mmol), 4-vinylpyridine (0.27 mL, 2.53 mmol), palladium acetate (14 mg, 0.06 mmol), and tri-*o*-tolylphosphine (0.12 mmol, 36 mg) in triethylamine (20 mL) and DMF (10 mL) was heated to 80 °C and stirred overnight under N_2. The reaction mixture was cooled to room temperature and extracted with DCM. The organic layer was washed with brine, dried over anhydrous sodium sulfate, and evaporated to dryness. The residue was purified by silica gel column chromatography to give 0.74 g (84% yield) of compound **S3** as a yellow solid. ^{1}H NMR (400 MHz, $CDCl_3$, δ): 8.55 (d, J = 5.6 Hz, 1H), 8.21 (s, 1H), 8.10 (d, J = 7.6 Hz, 1H), 7.67 (dd, J = 8.8 Hz, 1.6 Hz, 1H), 7.55 (d, J = 8.4 Hz, 4H), 7.45 (m, 3H), 7.38 (m, 2H), 7.31 (d, J = 16.8 Hz, 2H), 7.25 (m, 1H), 7.14 (d, J = 16.0 Hz, 1H), 7.06 (d, J = 16.4 Hz, 1H), 4.51 (t, J = 6.4 Hz, 2H), 3.86 (t, J = 6.4 Hz, 2H), 3.51 (m, 2H), 3.42 (m, 2H), 3.30 (s, 3H). ^{13}C NMR (100 MHz, $CDCl_3$, δ): 150.2, 144.7, 140.9, 140.5, 138.5, 134.7, 132.8, 130.3, 128.5, 127.4, 126.6, 125.9, 125.3, 124.5, 123.3, 122.9, 120.7, 120.3, 119.3, 118.7, 109.2, 109.0, 71.9, 70.8, 69.2, 59.0, 43.2. HRMS (MALDI-TOF) m/z: $[M]^+$ calcd for $C_{32}H_{30}N_2O_2$ 475.2254, found 475.2266. Anal. Calcd for $C_{32}H_{30}N_2O_2$: C, 80.98; H, 6.37; N, 5.90. Found: C, 80.76; H, 6.28; N, 5.82.

Compound ***3b***. To a solution of compound **2a** (3.58 g, 11.7 mmol) in dry THF was added sodium hydride (309 mg, 12.9 mmol). The resulting mixture was stirred for 40 min at 45 °C and diethyl 4-benzylphosphonate (1.27 g, 3.9 mmol) in THF was added via syringe. The solution mixture was then heated to reflux and stirred overnight. The reaction mixture was cooled to room temperature and quenched with aqueous ammonium chloride. The organic layer was separated and dried over anhydrous sodium sulfate. The solvent was removed in vacuo, and the residue was recrystallized from dichloromethane and hexane to give 2.05 g (83% yield) of compound **3b** as a brown solid. ^{1}H NMR (400 MHz, $CDCl_3$, δ): 8.20 (s, 2H), 7.63 (dd, J = 8.4 Hz, 1.2 Hz, 2H), 7.47 (d, J = 8.4 Hz, 4H), 7.41 (m, 6H), 7.27 (d, J = 16.0 Hz, 2H), 7.06 (d, J = 16.0 Hz, 2H), 4.48 (t, J = 6.0 Hz, 2H), 3.86 (t, J = 6.4 Hz, 2H), 3.50 (m, 2H), 3.41 (m, 2H), 3.29 (s, 3H). ^{13}C NMR (100 MHz, $CDCl_3$, δ): 140.8, 136.7, 131.7, 130.1, 128.6, 127.6, 124.9, 124.7, 123.2, 120.6, 118.6, 109.3, 71.9, 70.8, 69.2, 59.0, 43.3. HRMS (MALDI-TOF) m/z: $[M]^+$ calcd for $C_{33}H_{29}Br_2NO_2$ 629.0560, found 629.0569.

Compound ***V3***. A mixture of compound **3b** (1.85 g, 2.9 mmol), 4-vinylpyridine (1.25 mL, 11.7 mmol), palladium acetate (33 mg, 0.15 mmol), and tri-*o*-tolylphosphine (91 mg, 0.30 mmol) in triethylamine (40 mL) and DMF (20 mL) was heated to 80 °C and stirred overnight under N_2. The reaction mixture was cooled to room temperature and extracted with DCM. The organic layer was washed with brine, dried over anhydrous sodium sulfate, and evaporated to dryness. The residue was purified by silica gel column chromatography to give 1.47 g (74% yield) of compound **V3** as a yellow solid. ^{1}H NMR (400 MHz, $CDCl_3$, δ): 8.56 (d, J = 6.0 Hz, 4H), 8.24 (d, J = 1.2 Hz, 4H), 7.67 (dd, J = 8.4 Hz, 1.2 Hz, 2H), 7.55 (d, J = 8.4 Hz, 8H), 7.44 (d, J = 8.4 Hz, 2H), 7.37 (m, 6H), 7.30 (d, J = 16.4 Hz, 2H), 7.16 (d, J = 16.0 Hz, 2H), 7.02 (d, J = 16.4 Hz, 2H), 4.50 (t, J = 6.4 Hz, 2H), 3.88 (t, J = 6.0 Hz, 2H), 3.51 (m, 2H), 3.42 (m, 2H), 3.30 (s, 3H). ^{13}C NMR (100 MHz, $CDCl_3$, δ): 150.2, 144.7, 140.9, 138.4, 134.8, 132.8, 130.1, 128.9, 127.4, 126.6, 125.6, 125.4, 124.8, 123.3, 120.7, 118.7, 109.4, 71.9, 70.9, 69.3, 59.1, 43.4. HRMS (MALDI-TOF) m/z: $[M]^+$ calcd for $C_{47}H_{41}N_3O_2$ 679.3193, found 679.3211. Anal. Calcd for $C_{47}H_{41}N_3O_2$: C, 83.03; H, 6.08; N, 6.18. Found: C, 82.93; H, 5.95; N, 5.96.

■ ASSOCIATED CONTENT

Supporting Information

Absorption and fluorescence spectra of chromophores **S2**, **S3**, **V2**, and **V3** in toluene and $CHCl_3$; NMR titration of **S3** and **V2**; plots of normalized change of chemical shift versus Pb^{2+} equivalents for **S2**, **S3**, and **V2**; Job's plots of change of proton chemical shifts; CV titrations; absorption spectra of **S2** upon addition of Na^+ metal ions in acetonitrile; fluorescence spectra of **S2**, **S3**, **V2**, and **V3** upon addition of Na^+ in acetonitrile; fluorescence spectral changes for **S2**, **S3**, and **V2** upon addition of metal ions in acetonitrile; and ^{1}H and ^{13}C NMR spectra of **S2**, **V2**, **3a**, **S3**, **3b**, and **V3**. This material is available free of charge via the Internet at http://pubs.acs.org.

■ AUTHOR INFORMATION

Corresponding Authors

*Fax: (+86)-571-28862271. E-mail: xjfeng@hznu.edu.cn.
*Fax: (+86)-571-28862271. E-mail: zhengxu@hznu.edu.cn.
*Fax: (+852)-34117348. E-mail: mswong@hkbu.edu.hk.

Notes

The authors declare no competing financial interest.

■ ACKNOWLEDGMENTS

This work was supported by the General Research Fund (GRF) (HKBU 202408), the Hong Kong Research Grant Council, SAR Hong Kong, and the Zhejiang Provincial Natural Science Foundation of China (ZJNSF LY13E030005). We are grateful to the Computational Center for Molecular Design of Organosilicon Compounds at Hangzhou Normal University for provision of the SGI Altix 450 server.

■ REFERENCES

(1) Zhao, Y. P.; Wu, L. Z.; Si, G.; Liu, Y.; Xue, H.; Zhang, L. P.; Tung, C. H. *J. Org. Chem.* **2007**, *72*, 3632−3639.
(2) Xue, H.; Tang, X. J.; Wu, L. Z.; Zhang, L. P.; Tung, C. H. *J. Org. Chem.* **2005**, *70*, 9727−9734.
(3) Li, H. Y.; Gao, S.; Xi, Z. *Inorg. Chem. Commun.* **2009**, *12*, 300−303.
(4) Que, E. L.; Domaille, D. W.; Chang, C. J. *Chem. Rev.* **2008**, *108*, 1517−1549.
(5) Yang, R. H.; Chan, W. H.; Lee, W. M.; Xia, P. F.; Zhang, H. K.; Li, K. A. *J. Am. Chem. Soc.* **2003**, *125*, 2884−2885.
(6) Yao, J.; Dou, W.; Qin, W. W.; Liu, W. S. *Inorg. Chem. Commun.* **2009**, *12*, 116−118.
(7) Zhu, M.; Yuan, M. J.; Liu, X. F.; Xu, J. L.; Lv, J.; Huang, C. S.; Liu, H. B.; Li, Y. L.; Wang, S.; Zhu, D. B. *Org. Lett.* **2008**, *10*, 1481−1484.
(8) Sirilaksanapong, S.; Sukwattanasinitt, M.; Rashatasakhon, P. *Chem. Commun.* **2012**, *48*, 293−295.
(9) Wang, M.; Wang, J.; Xue, W.; Wu, A. *Dyes Pigm.* **2013**, *97*, 475−480.
(10) Metivier, R.; Leray, I.; Valeur, B. *Chem. Commun.* **2003**, 996−997.
(11) Metivier, R.; Leray, I.; Valeur, B. *Chem.—Eur. J.* **2004**, *10*, 4480−4490.
(12) Kim, J. S.; Kim, H. J.; Kim, H. M.; Kim, S. H.; Lee, J. W.; Kim, S. K.; Cho, B. R. *J. Org. Chem.* **2006**, *71*, 8016−8022.
(13) Kumar, M.; Babu, J. N.; Bhalla, V.; Kumar, R. *Sens. Actuators, B* **2010**, *144*, 183−191.
(14) McClure, D. S. *J. Chem. Phys.* **1952**, *20*, 682−686.
(15) Varnes, A. W.; Dodson, R. B.; Whery, E. L. *J. Am. Chem. Soc.* **1972**, *94*, 946−950.
(16) Otsubo, T.; Aso, Y.; Takimiya, K. *Adv. Mater.* **1996**, *8*, 203−211.
(17) Wallis, J. D.; Griffiths, J. P. *J. Mater. Chem.* **2005**, *15*, 347−365.
(18) Balandier, J.-Y.; Belyasmine, A.; Sallé, M. *Eur. J. Org. Chem.* **2008**, 269−276.

(19) Ni, X.-L.; Wang, S.; Zeng, X.; Tao, Z.; Yamato, T. *Org. Lett.* **2011**, *13*, 552−555.
(20) Fitilis, I.; Fakis, M.; Polyzos, I.; Giannetas, V.; Persephonis, P.; Vellis, P.; Mikroyannidis, J. *Chem. Phys. Lett.* **2007**, *447*, 300−304.
(21) Yang, J. X.; Wang, C. X.; Li, L.; Lin, N.; Tao, X. T.; Tian, Y. P.; Zhao, X.; Jiang, M. H. *Chem. Phys.* **2009**, *358*, 39−44.
(22) Li, S. L.; Wu, J. Y.; Tian, Y. P.; Tang, Y. W.; Jiang, M. H.; Fun, H. K.; Chantrapromma, S. *Opt. Mater.* **2006**, *28*, 897−903.
(23) Zhou, H.-P.; Tian, Y.-P.; Wu, J.-Y.; Zhang, J.-Z.; Li, D.-M.; Zhu, Y.-M.; Hu, Z.-J.; Tao, X.-T.; Jiang, M.-H.; Xie, Y. *Eur. J. Inorg. Chem.* **2005**, 4976−4984.
(24) Grigoras, M.; Vacareanu, L.; Ivan, T.; Catargiu, A. M. *Dyes Pigm.* **2013**, *98*, 71−81.
(25) Liu, X.; Sun, Y.; Zhang, Y.; Zhao, N.; Zhao, H.; Wang, G.; Yu, X.; Liu, H. *J. Fluoresc.* **2011**, *21*, 497−506.
(26) Walsh, J.; Mandal, K. *J. Org. Chem.* **1999**, *64*, 6102−6105.
(27) Mao, M.; Ren, M.-G.; Song, Q.-H. *Chem.—Eur. J.* **2012**, *18*, 15512−15522.
(28) Feng, X. J.; Wu, P. L.; Bolze, F.; Leung, W. C.; Li, K. F.; Mak, N. K.; Kwong, W. J.; Nicoud, J.-F.; Cheah, K. W.; Wong, M. S. *Org. Lett.* **2010**, *12*, 2194−2197.
(29) Cannors, K. A. *Binding Constants: The Measurement of Molecular Complex Stability*; Wiley: New York, 1987.
(30) Frisch, M. J.; Trucks, G. W.; Schlegel, H. B.; Scuseria, G. E.; Robb, M. A.; Cheeseman, J. R.; Scalmani, G.; Barone, V.; Mennucci, B.; Petersson, G. A.; Nakatsuji, H.; Caricato, M.; Li, X.; Hratchian, H. P.; Izmaylov, A. F.; Bloino, J.; Zheng, G.; Sonnenberg, J. L.; Hada, M.; Ehara, M.; Toyota, K.; Fukuda, R.; Hasegawa, J.; Ishida, M.; Nakajima, T.; Honda, Y.; Kitao, O.; Nakai, H.; Vreven, T.; Montgomery, J. A., Jr.; Peralta, J. E.; Ogliaro, F.; Bearpark, M.; Heyd, J. J.; Brothers, E.; Kudin, K. N.; Staroverov, V. N.; Kobayashi, R.; Normand, J.; Raghavachari, K.; Rendell, A.; Burant, J. C.; Iyengar, S. S.; Tomasi, J.; Cossi, M.; Rega, N.; Millam, N. J.;Klene, M.; Knox, J. E.; Cross, J. B.; Bakken, V.; Adamo, C.; Jaramillo, J.; Gomperts, R.; Stratmann, R. E.; Yazyev, O.; Austin, A. J.; Cammi, R.; Pomelli, C.; Ochterski, J. W.; Martin, R. L.; Morokuma, K.; Zakrzewski, V. G.; Voth, G. A.; Salvador, P.; Dannenberg, J. J.; Dapprich, S.; Daniels, A. D.; Farkas, Ö.; Foresman, J. B.; Ortiz, J. V.; Cioslowski, J.; Fox, D. J. *Gaussian 09*, revision C.01; Gaussian, Inc.: Wallingford, CT, 2010.